Z. Phys. D 29, 209–212 (1994)

ZEITSCHRIFT
FÜR PHYSIK D

Characterization of the $X^2\Sigma_u^+$ state of $^7Li_2^-$ via negative ion photoelectron spectroscopy

H.W. Sarkas, S.T. Arnold, J.H. Hendricks, V.L. Slager, K.H. Bowen

Department of Chemistry, Johns Hopkins University, Baltimore, MD 21218, USA

Received: 25 June 1993 / Final version: 25 September 1993

Abstract. The negative ion photoelectron spectrum of $^7Li_2^-$ is reported at 488 nm (2.540 eV). Three electronic bands are observed in this spectrum and are assigned to the following photodetachment transitions: $^7Li_2$, $X^1\Sigma_g^+ + e^- \leftarrow {}^7Li_2^-$, $X^2\Sigma_u^+$; $^7Li_2$, $a^3\Sigma_u^+ + e^- \leftarrow {}^7Li_2^-$, $X^2\Sigma_u^+$; and $^7Li_2$, $A^1\Sigma_u^+ + e^- \leftarrow {}^7Li_2^-$, $X^2\Sigma_u^+$. The electron affinity of $^7Li_2$ is determined to be 0.437 ± 0.009 eV, leading to an anion dissociation energy, D_0, of 0.865 ± 0.022 eV for the ground state of $^7Li_2^-$. A Franck-Condon analysis of the $^7Li_2$, $X^1\Sigma_g^+ + e^- \leftarrow {}^7Li_2^-$, $X^2\Sigma_u^+$ band yields the following spectroscopic constants for the ground state of $^7Li_2^-$: $B_e = 0.502 \pm 0.005$ cm^{-1}, $r_e = 3.094 \pm 0.015$ Å, and $\omega_e = 232 \pm 35$ cm^{-1}.

PACS: 33.60.−q; 35.20.Dp; 35.20.Gs; 35.20.Vf.

1. Introduction

Lithium dimer is the smallest homonuclear diatomic molecule capable of forming a stable negative ion. Although H_2 is isoelectronic to Li_2, the $X^2\Sigma_u^+$ state of H_2^- is not stable with respect to autodetachment and thus exists only as a resonance [1]. In addition, He_2^- has been observed only as a high-lying metastable in a $^4\Pi_u$ state [2–4]. Due to its fundamental nature, Li_2^- has been the subject of numerous theoretical studies, nearly all of which predict a bound ground state of $^2\Sigma_u^+$ symmetry [5–13]. Despite this theoretical interest, experimental information regarding the bound nature of this species has thus far been limited to mass spectrometric observations of Li_2^- [14, 15]. Other information regarding the interaction of electrons with Li_2 has been provided by dissociative electron attachment studies and the observation of electron scattering resonances [16, 17]. Here, we present the photoelectron spectrum of Li_2^- along with spectroscopic constants for the $X^2\Sigma_u^+$ Li_2^- ground state which were extracted from a Franck-Condon analysis of the photoelectron spectrum.

2. Experimental

Negative ion photoelectron spectroscopy is conducted by crossing a mass selected beam of negative ions with a fixed-frequency photon beam and energy analyzing the resultant photodetached electrons. Our negative ion photoelectron spectrometer has been described previously [18]. Briefly, anions are generated in a supersonic expansion cluster ion source, skimmed, and transported through a series of ion optical components on through an $\mathbf{E} \times \mathbf{B}$ Wien velocity filter where they are mass selected. After being focused into the field-free, collision-free ion/photon interaction region, the mass selected cluster ion beam is crossed with the intracavity photon beam of an argon ion laser operated at visible wavelengths. A small solid angle of the resulting photodetached electrons is accepted into the input optics of a magnetically shielded, hemispherical electron energy analyzer, where the electrons are energy analyzed and

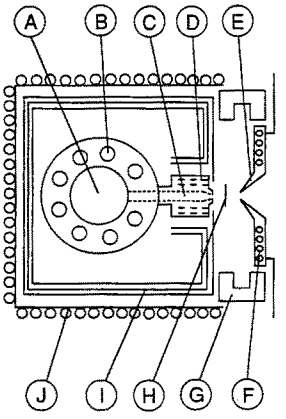

Fig. 1. Schematic diagram of our high temperature supersonic expansion ion source. The components of the source are: (A) oven reservoir, (B) oven reservoir heaters, (C) nozzle, (D) nozzle heaters, (E) high temperature skimmer, (F) skimmer heaters, (G) magnets, (H) ionizing filament, (I) radiation shields, and (J) copper cold shield

counted. The photoelectron spectra of lithium dimer anion were recorded with an instrumental resolution of 30 meV at photon energies of 2.540 eV and 2.707 eV.

Beams of lithium dimer anion were produced using a specially designed high temperature seeded beam supersonic expansion ion source. A schematic diagram of the source is presented in Fig. 1. The main portion of the source is a high temperature oven consisting of separately heated reservoir and nozzle sections. Both sections are constructed of stainless steel (type 304) with evenly spaced holes in each for inserting heaters. The heaters consist of tantalum wires (0.5 mm diameter) insulated using high purity multi-hole ceramic rods (99.8% Al_2O_3, McDanel). High purity lithium metal (99.9% Aldrich) is heated in the reservoir to 1300 K, yielding approximately 50 torr of lithium vapor which is coexpanded into high vacuum with 50–150 torr of preheated high purity argon (99.99%) through a 0.15 mm diameter orifice in the nozzle section (maintained at 1350 K). The use of higher carrier gas pressures was found to induce severe beam instabilities and to drastically reduce ion currents. A negatively biased hot thoriated iridium filament injects low energy electrons directly into the expanding lithium-argon jet in the presence of a predominantly axial magnetic field which is used to enhance ion production. The beam is skimmed by a high temperature conical skimmer and ions are extracted into the spectrometer. The stainless steel skimmer is heated in a similar manner to the oven, and its design allows for temperatures of 1000 K to be maintained at the tip. This was found to be a necessary condition for preventing occlusion of the skimmer hole. Under these conditions, typical currents measured downstream of the ion-photon interaction region ranged from 10–60 pA for Li_2^-, and a representative mass spectrum of $Li_{n=1-3}^-$ is presented in Fig. 2.

3. Results and discussion

The photoelectron spectrum of $^7Li_2^-$, recorded using 2.540 eV photons, is presented in Fig. 3. This spectrum was recorded over about 3.5 hours with a $^7Li_2^-$ current of 10–60 pA and a circulating laser power of 120 W. The absolute kinetic energy scale was calibrated by recording $^7Li^-$ spectra immediately before and after the $^7Li_2^-$ spectrum, and comparing the measured electron binding energies to the established value for the electron affinity of the lithium atom [19, 20]. The $^7Li_2^-$ spectrum is highly structured, with individual peaks arising due to photodetachment transitions between the $X^2\Sigma_u^+$ ground state of $^7Li_2^-$ and the ground and energetically accessible low-lying excited electronic states of $^7Li_2$. All of the features in this spectrum have been assigned, guidance having been provided by available theoretical results and optical data [21–25]. Assignments of the photodetachment transitions giving rise to each feature in the photoelectron spectrum are given in Fig. 3 above each corresponding spectral feature. The lowest electron binding energy (EBE) feature corresponds to the photodetachment transition from the $X^2\Sigma_u^+$ ground state of $^7Li_2^-$ to the $X^1\Sigma_g^+$ ground state of $^7Li_2$. The spectral width of this feature is a consequence of a vibrational progression, and the appearance of several distinct vibrational features in this band has allowed a detailed analysis to be carried out which will be discussed below. The next highest EBE feature in the spectrum is due to the $^7Li_2$, $a^3\Sigma_u^+ + e^- \leftarrow {}^7Li_2^-$, $X^2\Sigma_u^+$ transition. A comparison of the determined spectroscopic constants for the $X^2\Sigma_u^+$ state of $^7Li_2^-$ with high level calculations [22]

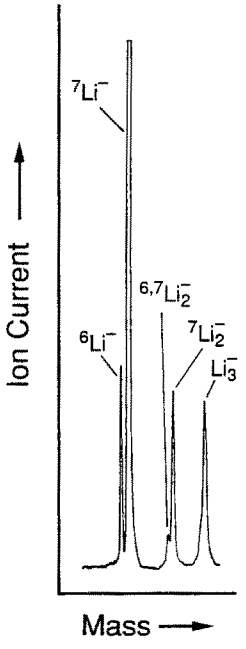

Fig. 2. A mass spectrum of $Li_{n=1-3}^-$. This spectrum was recorded under high ion transmission conditions using a relatively low Wien filter electric field setting

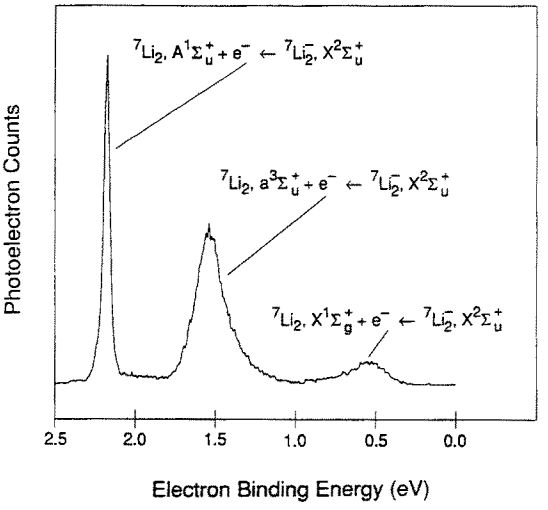

Fig. 3. The photoelectron spectrum of $^7Li_2^-$ recorded using 2.540 eV photons. Assignments for the photodetachment transitions giving rise to each spectral feature are designated on the figure

on the $a^3\Sigma_u^+$ state of $^7Li_2$ suggests that the spectral shape of this feature on its low EBE side reflects access of the weakly bound portion of the $a^3\Sigma_u^+$ potential while the shape of the high EBE side reflects access to the repulsive portion of this potential at smaller internuclear distances. The highest EBE feature in the spectrum arises due to the $^7Li_2$, $A^1\Sigma_u^+ + e^- \leftarrow {}^7Li_2^-$, $X^2\Sigma_u^+$ transition. The width of this feature implies that the equilibrium bond distances of the $X^2\Sigma_u^+$ state of $^7Li_2^-$ and the $A^1\Sigma_u^+$ state of $^7Li_2$ are very similar. The photoelectron spectrum of $^7Li_2^-$ displays the same qualitative features as the spectra of the heavier homonuclear alkali dimer anions which we have reported previously [26], with one exception. At the photon energies employed in this study and in our previous work, the M_2, $b^3\Pi_u + e^- \leftarrow M_2^-$, $X^2\Sigma_u^+$ transitions should be energetically accessible for all the alkali dimer anions. The feature corresponding to this transition appears clearly as a small shoulder on the low EBE side of the M_2, $A^1\Sigma_u^+ + e^- \leftarrow M_2^-$, $X^2\Sigma_u^+$ transition in the spectra of Na_2^-, K_2^-, Rb_2^-, and Cs_2^-. In the photoelectron spectrum of Li_2^-, however, no such feature is observed. Since the M_2, $b^3\Pi_u + e^- \leftarrow M_2^-$, $X^2\Sigma_u^+$ transition is a two electron process, its apparent absence in the spectrum of Li_2^- may indicate that contributions of π orbital-containing configurations to the total ground state configuration of Li_2^- are significantly less than those to the total ground state configurations of the heavier alkali dimer anions.

The adiabatic electron affinity of lithium dimer was determined by two approaches, both of which were found to yield the same result. In one approach, an accurate determination of the adiabatic electron affinity of $^7Li_2$ was made by subtracting the energy of the $A^1\Sigma_u^+(v''=0) \rightarrow X^1\Sigma_g^+(v'=0)$ optical transition [25] in $^7Li_2$ from the EBE of the center of the spectral feature corresponding to the $^7Li_2$, $A^1\Sigma_u^+ + e^- \leftarrow {}^7Li_2^-$, $X^2\Sigma_u^+$ transition in the photoelectron spectrum of $^7Li_2^-$. This band appears as a single narrow feature in the photoelectron spectrum. A consideration of the vibrational frequency of the $A^1\Sigma_u^+$ state of $^7Li_2$ [24, 25] implies that this band must be dominated by a single vibrational feature corresponding to the $^7Li_2$, $A^1\Sigma_u^+(v'=0) + e^- \leftarrow {}^7Li_2^-$, $X^2\Sigma_u^+(v''=0)$ photodetachment transition (along with much smaller contributions from other $\Delta v=0$ photodetachment transitions). Thus, subtracting the $A^1\Sigma_u^+(v'=0) \rightarrow X^1\Sigma_g^+(v''=0)$ transition energy for $^7Li_2$, from our measured $^7Li_2$, $A^1\Sigma_u^+(v'=0) + e^- \leftarrow {}^7Li_2^-$, $X^2\Sigma_u^+(v''=0)$ transition energy (EBE) gives the energy difference between the $X^2\Sigma_u^+(v''=0)$ state of $^7Li_2^-$ and the $X^1\Sigma_g^+(v'=0)$ state of $^7Li_2$, i.e. the adiabatic electron affinity. In order to ascertain that our measurement of the $^7Li_2$, $A^1\Sigma_u^+(v'=0) + e^- \leftarrow {}^7Li_2^-$, $X^2\Sigma_u^+(v''=0)$ transition energy was not affected by the electron transmission function of our energy analyzer, we also recorded the spectrum of $^7Li_2^-$ at 457.9 nm (2.707 eV). The measured EBE's of the peak centers for this transition measured using 2.707 eV and 2.540 eV photons agreed to within 1 meV, which lies well within the error limits for determining absolute electron binding energies in this experiment. The rotational energy correction [27] to the $^7Li_2$, $A^1\Sigma_u^+(v'=0) + e^- \leftarrow {}^7Li_2^-$, $X^2\Sigma_u^+(v''=0)$ transition energy was also considered. Due to the very similar equilibrium bond distances, and thus similar rotational constants of the $X^2\Sigma_u^+$ state of $^7Li_2^-$ and the $A^1\Sigma_u^+$ state of $^7Li_2$, the rotational energy correction here is negligible. In fact, using the spectroscopic constants determined in this study for the $X^2\Sigma_u^+$ state of $^7Li_2^-$ (see below) we estimate this correction to be less than 1 meV. Thus, the value for the adiabatic electron affinity of $^7Li_2$ determined here is 0.437 ± 0.009 eV. The stated uncertainty is chosen to account for all possible errors in absolute kinetic energy scale calibrations, errors in determining the energy scale compression factor, and errors in the peak fitting procedure. Our experimental value for the adiabatic electron affinity of $^7Li_2$ is in good agreement with several theoretical values [7–11]. Of course, the adiabatic electron affinity corresponds to the EBE of the $^7Li_2$, $X^1\Sigma_g^+(v'=0) + e^- \leftarrow {}^7Li_2^-$, $X^2\Sigma_u^+(v''=0)$ transition.

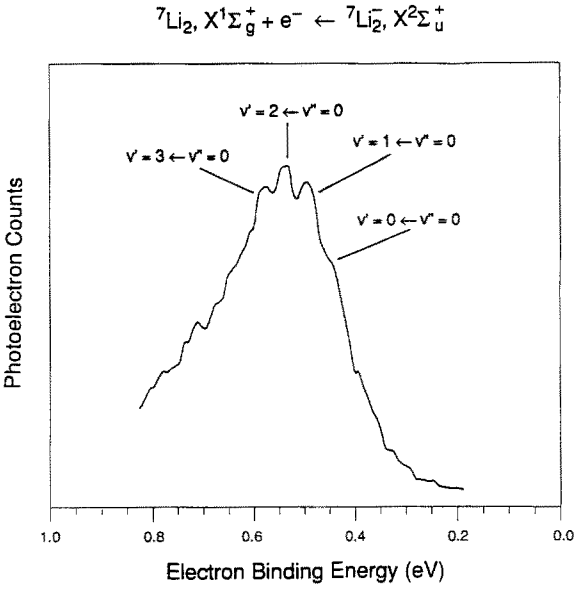

Fig. 4. A long integration time scan over the $^7Li_2$, $X^1\Sigma_g^+ + e^- \leftarrow {}^7Li_2^-$, $X^2\Sigma_u^+$ electronic band recorded using 2.540 eV photons. The assignments of several vibrational features in this band are designated on the figure, where ('') denotes an anion vibrational level and (') denotes a neutral vibrational level

Spectroscopic constants for the ground state of $^7Li_2^-$ were obtained by performing anharmonic Franck-Condon spectral simulations of the $^7Li_2$, $X^1\Sigma_g^+ + e^- \leftarrow {}^7Li_2^-$, $X^2\Sigma_u^+$ band. In order to facilitate this procedure, a long integration time scan was performed on this band using 2.540 eV photons, and this spectrum is shown in Fig. 4, along with assignments for several vibrational features. Simulations were generated using the known values of ω_e, $\omega_e x_e$, and r_e for $^7Li_2$ [24] and by varying the origin band position, the vibrational frequency, vibrational anharmonicity, equilibrium bond distance, and vibrational temperature of the anion. The simulated spectra were then compared to the empirical spectrum in a least squares sense. This procedure yielded an assignment of the vibrational features in this band as well as the spectroscopic constants for the ground state of $^7Li_2^-$. The

EBE of the ($v'=0 \leftarrow v''=0$) feature gave the adiabatic electron affinity by a second approach confirming that determined by the first method. The spectroscopic constants determined for $^7Li_2^-$ are: $B_e = 0.502 \pm 0.005$ cm^{-1}, $r_e = 3.094 \pm 0.015$ Å, and $\omega_e = 232 \pm 35$ cm^{-1}. The anion vibrational anharmonicity was not determined here since this quantity had no significant effect on the fit. In addition, a vibrational temperature of 280 K was determined for $^7Li_2^-$. Finally, using our experimentally determined value for the electron affinity of $^7Li_2$, the dissociation energy of $^7Li_2^-$ was determined via the following thermochemical cycle:

$$D_0[^7Li_2^-, X\,^2\Sigma_u^+] = D_0[^7Li_2, X\,^1\Sigma_g^+] + E.A.[^7Li_2] - E.A.[Li] \quad (1)$$

Using the recommended value for the dissociation energy of $^7Li_2$ [28] and the established literature value for the electron affinity of Li [19, 20], a value of 0.865 ± 0.022 eV was obtained for $D_0[^7Li_2^-, X\,^2\Sigma_u^+]$. This value along with the other spectroscopic constants for the $X\,^2\Sigma_u^+$ state of $^7Li_2^-$ are in good agreement with those determined in several theoretical investigations.

We wish to thank C.W. Bauschlicher, Jr., R.A. Bernheim, W. de Heer, J.L. Gole, D.M. Lindsay, H.H. Michels, T.M. Miller, E. Poliakoff and W.C. Stwalley for stimulating discussions, and G. Pisiello for his expert machining of our high temperature cluster ion source. We gratefully acknowledge the support of the National Science Foundation under Grant CHE-9007445. Grateful acknowledgement is made to the Donors of The Petroleum Research Fund, administered by the American Chemical Society, for partial support of this research.

References

1. Schulz, G.J.: Rev. Mod. Phys. **45**, 423 (1973)
2. Bae, Y.K., Coggiola, M.J., Peterson, J.R.: Phys. Rev. Lett. **52**, 747 (1984)
3. Kvale, T.J., Compton, R.N., Alton, G.D., Thompson, J.S., Pegg, D.J.: Phys. Rev. Lett. **56**, 592 (1986)
4. Michels, H.H.: Phys. Rev. Lett. **52**, 1413 (1984)
5. Blustin, P.H., Linnett, J.W.: J. Chem. Soc. Faraday Trans. 2 **70**, 826 (1974)
6. Andersen, E., Simons, J.: J. Chem. Phys. **64**, 4548 (1976)
7. Dixon, D.A., Gole, J.L., Jordan, K.D.: J. Chem. Phys. **66**, 567 (1977)
8. Partridge, H., Bauschlicher, C.W., Siegbahn, P.E.M.: Chem. Phys. Lett. **97**, 198 (1983)
9. Konowalow, D.D., Fish, J.L.: Chem. Phys. Lett. **104**, 210 (1984)
10. Sunil, K.K., Jordan, K.D.: Chem. Phys. Lett. **104**, 343 (1984)
11. Michels, H.H., Hobbs, R.H.,Wright, L.A.: Chem. Phys. Lett. **118**, 67 (1985)
12. Rao, B.K., Khanna, S.N., Jena, P.: In: Physics and chemistry of small clusters. Jena, P., Rao, B.K., Khanna, S.N., (eds.), p. 369. New York: Plenum Press 1987
13. Boustani, I., Koutecký, J.: J. Chem. Phys. **88**, 5657 (1988)
14. Middleton, R.: Negative Ion Cookbook. University of Pennsylvania: Philadelphia 1989
15. Sarkas, H.W., Arnold, S.T., Bowen, K.H.: (unpublished)
16. Miller, T.M., Kasdan, A., Bederson, B.: Phys. Rev. A **25**, 1777 (1982)
17. McGeoch, M.W., Schlier, R.E.: Phys. Rev. A **33**, 1708 (1986)
18. Coe, J.V., Snodgrass, J.T., Freidhoff, C.B., McHugh, K.M., Bowen, K.H.: J. Chem. Phys. **84**, 618 (1986)
19. Feldmann, D.: Z. Phys. A **277**, 19 (1976)
20. Mead, R.D., Stevens, A.E., Lineberger, W.C.: In: Gas phase ion chemistry. Bowers, M.T., (ed), Vol. III, p. 214. New York: Academic Press 1984
21. Konowalow, D.D., Olson, M.L.: J. Chem. Phys. **71**, 450 (1979)
22. Olson, M.L., Konowalow, D.D.: Chem. Phys. **21**, 393 (1977)
23. Konowalow, D.D., Rosenkrantz, M.E.: In: Metal Bonding and Interactions in High Temperature Systems. Gole, J.L., Stwalley, W.C., (eds.), p. 3. Washington, DC: American Chemical Society 1982
24. Huber, K.P., Herzberg, G.: Constants of Diatomic Molecules. p. 374. New York: Van Nostrand Reinhold 1979
25. Kusch, P., Hessel, M.M.: J. Chem. Phys. **67**, 586 (1977)
26. McHugh, K.M., Eaton, J.G., Lee, G.H., Sarkas, H.W., Kidder, L.H., Snodgrass, J.T., Manaa, M.R., Bowen, K.H.: J. Chem. Phys. **91**, 3792 (1989)
27. Celotta, R.J., Bennett, R.A., Hall, J.L., Siegel, M.W., Levine, J.: Phys. Rev. A **6**, 631 (1972)
28. Stwalley, W.C.: J. Chem. Phys. **65**, 2038 (1976)